

ภาคผนวก

Reprint ผลงานวิจัย

- [1] “Synthesis of spherical silica by sol-gel method and its application as catalyst support”, *AICHE*, 10 (2010), , 25-30, [Anirut Leksomboon and Bunjerd Jongsomjit^{*}], Impact factor (ISI) = -
- [2] “Investigation of Ti-Si composite oxide-supported cobalt catalysts over CO₂ hydrogenation, Journal of Natural Gas Conversion”, (in press) 2011, [Jakrapan Janlamool, Piyasan Praserttham, and Bunjerd Jongsomjit^{*}], Impact factor (ISI) = 1.345

Synthesis of Spherical Silica by Sol-Gel Method and Its Application as Catalyst Support

Anirut Leksomboon

Bunjerd Jongsomjit*

¹Department of Chemical Engineering, Faculty of Engineering, Chulalongkorn University, Bangkok, 10330, Thailand

*e-mail: bunjerd.j@chula.ac.th

In this present study, the spherical silica support was synthesized from tetraethyloxysilane (TEOS), water, sodium hydroxide, ethylene glycol and n-dodecyltrimethyl ammonium bromide ($C_{12}TMABr$). The particle size was controlled by variation of the ethylene glycol co-solvent weight ratio of a sol-gel method preparation in the range of 0.10 to 0.50. In addition, the particle size apparently increases with high weight ratio of co-solvent, but the particle size distribution was broader. The standard deviation of particle diameter is large when the co-solvent weight ratio is more than 0.35 and less than 0.15. However, the specific surface area was similar for all weight ratios ranging from 1000 to 1300 m²/g. The synthesized silica was spherical and has high specific surface area. The cobalt was impregnated onto the obtained silica to produce the cobalt catalyst used for CO₂ hydrogenation.

Keyword: Spherical silica, Sol-gel Method, Carbon dioxide hydrogenation

INTRODUCTION

Silica has been one of the main catalyst supports. The main topic of research into materials is uniformity of the shape, pore volume and the specific surface area [1, 2]. Among particles with all kinds of morphology, monodispersed silica spheres are very promising because of many applications in the area of catalysis and absorbents. The porous silica was synthesized and classified as mesoporous silica or submicroporous silica according to the diameter of the pore.

Silica sphere has been synthesized by various methods, such as using cationic surfactant under acidic condition, using nonionic surfactant as a template under static and acidic con-

dition, by addition of CTBA as co-surfactant or using the two step synthesis by pH adjustment and addition of small amount of fluoride as catalyst [3].

It has become possible to synthesize silica by the sol-gel method. The synthesis of monodispersed mesoporous silica spheres by modifying the Stöber procedure [4], with the further addition of the surfactant template, such as and alkyl amine. The synthesis has been extended to control the diameter and pore size of particle. However, the methods for preparation mesoporous silica spheres with uniform particle size and good dispersibility are still required.

Cobalt supported on silica has been subject of many studies. During the past 10 years,

cobalt based catalysts appear as the most popular system for Fischer-Tropsch and carbon oxide hydrogenation [5]. Many researches were investigated the metallic/bimetic support and promoter effect to the activity and selectivity of hydrocarbon formation. However, the effect of physical and chemical properties of support on the performance of Co catalysts in Fischer-Tropsch and carbon oxide synthesis still remains unclear [6].

The present work describes the synthesis of silica spheres with silica source of tetraethyloxysilane (TEOS) and n-dodecyltrimethyl ammonium bromide (C_{12} TMABr) as a surfactant template in a sol-gel method in alkali aqueous solution. The morphology and size of particle were controlled with the ethylene glycol co-solvent weight ratio of variation in the range of 0.10 to 0.50. The silica spheres were used as catalyst support of Co/SiO₂ and prepared by the incipient wetness technique. The silica sphere support and catalyst were characterization by X-ray diffraction (XRD), scanning electron microscopes (SEM), nitrogen physisorption (BET surface areas), CO chemisorptions isotherm. The activity and selectivity of catalyst were tested for the CO₂ hydrogenation when amounts of hydrocarbon product are generated.

EXPERIMENTAL

Material synthesis

Silica spheres (SiO₂) were prepared by the sol-gel method. C_{12} TMABr (>99%), TEOS (>99%) and cobalt (II) nitrate hexahydrate (98%) were purchased from Aldrich. Sodium hydroxide solution (1 M) and ethylene glycol were purchased from Merck. All gas in the reaction test was supplied by Thai Industrial Gas Co., Ltd.

In a typical synthesis procedure, 2.08 g of C_{12} TMABr and 3.74 ml of 1 M sodium hydroxide solution were dissolved in 500 g of ethylene glycol/water (25/75=w/w) solution (weight

ratio 0.25). Then, 3.12 g of TEOS was added to the solution. The composition of the reaction mixture was 1SiO₂:0.45 C_{12} TMABr:0.25NaOH:133ethylene glycol:1392H₂O. Then, stirred continuously at 293 K for 8 h. The white particles were filtered and washed with distilled water at least three times, and then dried the particles at 383 K for 48 h. The particles obtained were calcined in air at 823 K for 6 h. The silica spheres were also synthesized with different diameters by changing the weight ratio of ethylene glycol co-solvent in the range of 0.10 to 0.50 in the same sol-gel method.

The Co/SiO₂ catalysts were prepared by the incipient wetness impregnation with calcined SiO₂ and aqueous solution of Co (NO₃)₂ · 6H₂O. The Co loading was set to 20 wt.%. Then, dried at 383 K for 48 h overnight and calcined at 823 K for 5 h in air.

Characterization

Powder X-ray diffraction measurements were carried out with SIEMENS D-500 X-ray diffractometer using Cu-K_α radiation. The scan range was 20~80° with 0.04° step at the room temperature. Scanning electron microscopy (SEM) was obtained using JSM-5800VL (JEOL). The average particle diameter was calculated from the diameter of 50 particles observed in a SEM picture. BET surface areas were measured by nitrogen physisorption using a Micromeritics Chemisorb ASAP2620 automatic system at 77 K. The specific surface area was estimated by the BET method. The pore diameter and the pore volume were calculated from desorption branches using the Barrett-Joyner-Halenda (BJH) method. CO chemisorptions isotherms were measured at 303 K. The reactor was loaded with 0.5-1.0 g of catalyst using Micromeritics pulse 2750. Analyst of the catalysts was reduced in H₂ at 623 K for 3 h.

The activity test

The activity and selectivity of catalyst were tested in CO₂ hydrogenation. The stainless

RESULTS AND DISCUSSION

Silica spheres with sol-gel method

The SEM images of the representative sample are shown in Fig 1. The sample exhibited good spherical morphology in all co-solvent ratios. The synthetic results of the silica spheres as the variation of co-solvent ratio are listed in Table 1. The higher weight ratio of the co-solvent was changed to the size control of particle. The average particle decreased when the co-solvent weight ratio was reduced. However, the size distribution uniformity was poor with the co-solvent out of range 0.15 to 0.30. All of silica spheres have high specific surface area ranging from 1000 to 1300 m²/g. The pore size and pore volume of the silica spheres prepared using different weight ratio of co-solvent were similar in the narrow range. When the weight ratio of co-solvent was reduced until 0.1, the silica sphere led to increase the surface area, but the mean pore diameter was lower than other sample. However, the weight ratio of ethylene glycol hardly affected on the uniform and structure of silica sphere.

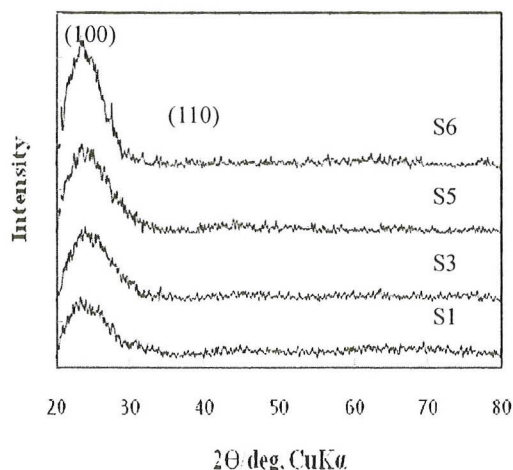


Figure 2. XRD Patterns of Spherical Silica

The small angle X-ray diffraction patterns of the sample exhibited one single broad at (100) plane in all particles. Respectively, the broad peak was small shifted to the higher angle and

higher order peaks when the diameter of particle was changed to the larger one. The representative XRD patterns are depicted in Fig.2

Cobalt-based silica sphere (Co/SiO₂)

The impregnation and calcination procedures were applied for catalyst preparation in the same Co loading. The catalyst was maintained the spherical morphology and constant particle size nearly as the support particle. The specific surface area of catalyst was reduced about 25 percentage of the support surface area as same as the pore volume, but the mean pore diameter of catalyst was not deviated value. The SEM picture was confirmed the shape and diameter of the catalyst in the Fig.3. The homogeneity and dispersibility of catalyst was obtained by SEM-EDS in the Fig 4. The dispersibility of catalyst on spherical silica is good and smoothness.

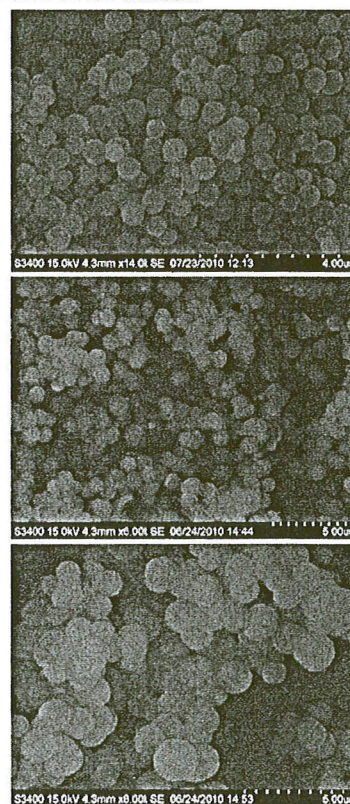


Figure 3. SEM images of various catalysts sample, the name of which are donated in Table 2.

Table 2. The CO Chemisorption of CO/SiO₂

Catalyst	Loading on support	CO Chemisorp (μmole CO/g catalyst)	Active site (molecules/g catalyst)	Dispersion (%)	CO Chemisorp/BET Surface Area (mole CO/m ²)
C1	S1	29.38	1.77E+19	0.87	0.0298
C2	S2	26.07	1.57E+19	0.77	0.0265
C3	S3	26.89	1.62E+19	0.79	0.0276
C4	S4	26.63	1.60E+19	0.74	0.0284
C5	S5	26.06	1.57E+19	0.77	0.0261
C6	S6	26.48	1.59E+19	0.78	0.0265
C7	S7	26.21	1.58E+19	0.78	0.0271

Table 3. Conversion and selectivity of Co/SiO₂ catalyst in CO₂ hydrogenation

Catalyst	CO ₂ Conversion (%)		Rate of reaction (mol CO ₂ /(g cat. h))	CH ₄ Selectivity (%)	CO Selectivity (%)
	Initial	Steady state			
C1	9.50	9.11	4.13E-2	64.20	35.80
C2	10.40	10.42	5.58E-2	78.05	21.95
C3	22.79	17.60	9.75E-2	87.25	12.75
C4	24.51	23.53	14.27E-2	90.84	9.16
C5	26.86	20.00	12.21E-2	91.73	8.27
C6	21.63	21.50	12.73E-2	87.27	12.73
C7	20.39	21.07	12.46E-2	90.20	9.80

The cobalt catalyst was a crystalline, evaluated by XRD. The characteristic sharp peak of cobalt was appeared in XRD patterns. The cobalt crystallite size of catalyst C1 was the largest and decreased crystallinity due to the lower surface area. The representative XRD patterns are depicted in Fig.5

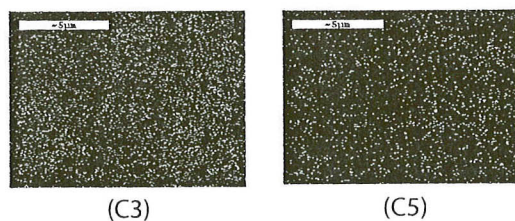
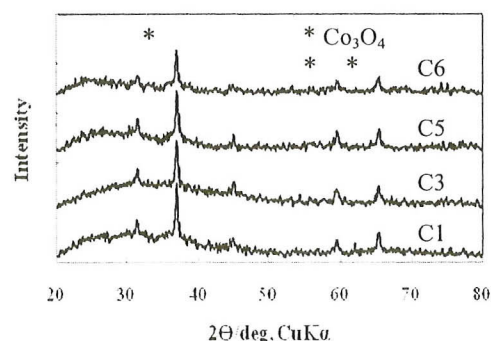
**Figure 4.** SEM-EDS images of catalysts C3 and C5

Table 2 summarizes the CO chemisorption result of catalyst. All samples exhibited high active sites. The chemisorptions results show the similar μmole of CO that can be absorbed per gram catalyst. The catalyst C1 was represented the different performance in the chemisorptions and dispersion percentage from other samples because it had larger specific surface area.

**Figure 5.** XRD patterns of Co/SiO₂

The activity test

The conversion and selectivity of cobalt-based silica sphere catalyst in CO₂ hydrogenation are shown in the Table 3. The initial state was tested around 5 min after started reaction and the steady-state was determined the average result within 3 to 6 h after started reaction. The primary major product in CO₂ hydrogenation of Co/SiO₂ catalyst is methane and small ethane is a secondary product of reaction. The carbon monoxide intermediate was generated from the reverse water-gas

steel fixed bed reactor (i.d. 10 mm) was used with 0.8–1.2 g of catalyst loading into the reactor and operated in an up flow mode with the bed help between quartz wool plugs. After the catalyst was reduced in H_2 at 623 K for 3 h under flow rate of 50 ml min^{-1} , the temperature was decreased to the reaction temperature at 493 K and H_2 gas was purged with high purify argon at the flow rate of 8.8 ml min^{-1} . The CO_2/H_2 ($8.8\%CO_2$) reactant was passed through the reactor at the flow rate 21.3 ml min^{-1} to

combine the argon gas. The reaction products were analyzed by gas chromatography (Shimatzu GC14B) with a VZ10 column and flame ionization detector (FID). The remainder reactant and carbon monoxide intermediate was detected by gas chromatography (Shimatzu GC8B) with a Molecular sieve 5A column and thermal conductivity detector (TCD). The reaction was analyzed not less than 6 h for the steady-state reaction.

Table 1. Properties of representative spherical silica

Sample lume	Weight ratio of Ethylene glycol	Average particle diameter [μm]	Standard deviation [%]	Specific surface area [m^2/g]	Mean pore diameter [nm]	Pore vo- lume [cm^3/g]
S1	0.10	0.58	21	1335	2.24	0.54
S2	0.15	0.68	9	1153	2.45	0.56
S3	0.20	0.74	5	1125	2.53	0.46
S4	0.25	1.04	5	1105	2.56	0.46
S5	0.30	1.16	28	1075	2.54	0.52
S6	0.40	1.33	30	1085	2.38	0.56
S7	0.50	1.64	35	1092	2.45	0.40

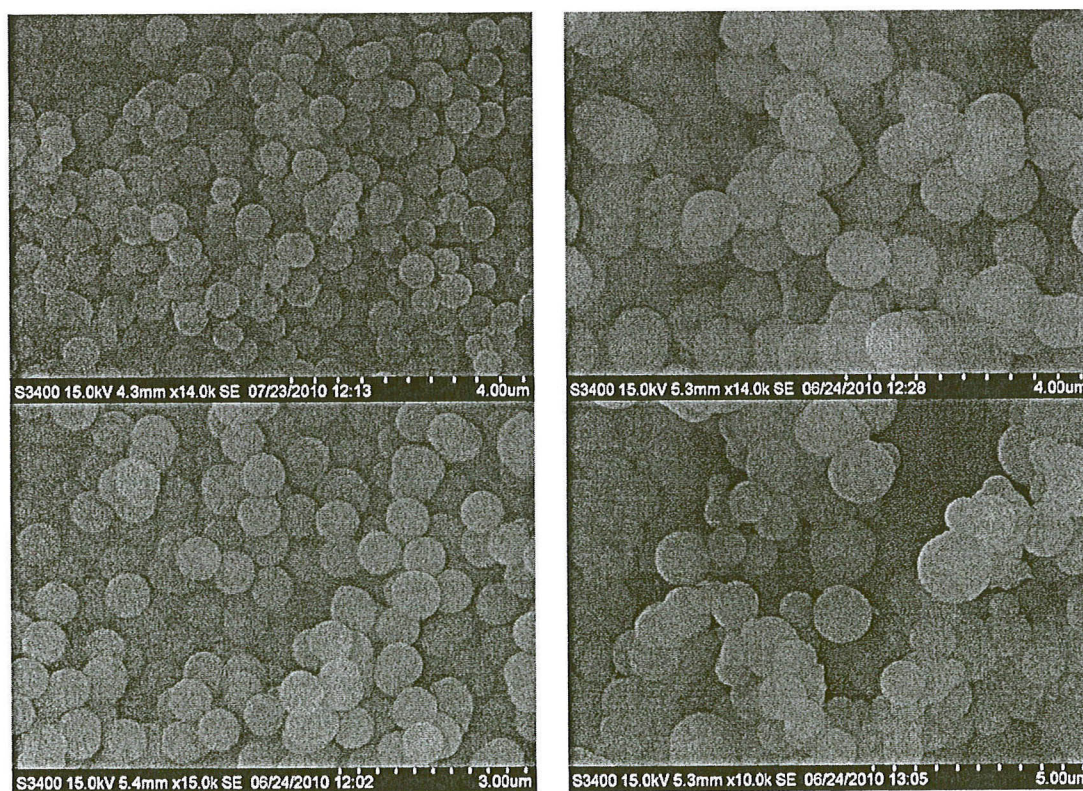


Figure 1. SEM images of various samples, the name of which are denoted in Table 1.

shift reaction (RWGS) used to calculate the rate of reaction and selectivity. Based on results, the catalyst has nearly CO₂ conversion between initial and steady state and the conversion was larger when the particle of support increased to diameter of 1.0 μm . The rate of reaction and selectivity exhibited the result as same as the conversion. However, the catalyst C1 has the highest active site, but it conducted poor conversion, selectivity and rate of reaction. The particle size distribution and uniform shape affected on the reaction. The CO selectivity is inverse value. The intermediate was generated from RWGS, but not to be used in the hydrogenation. The catalyst number C4 and upper exhibited good results in the activity test, perhaps due to a very small particle was pressed in the reactor against the adsorption and increased pressure in the reactor.

Furthermore, catalyst C1 and C2 having a small particle size and broad size distribution will be investigated more in the near future.

CONCLUSION

In summary, the sol-gel method was successfully used to synthesize the spherical silica from TEOS and C₁₂TMABr as a surfactant template. The particle has a good shape and morphology. The particle diameter was controlled by changing the weight ratio of ethylene glycol co-solvent. The uniformity of particle diameter has a high standard deviation, when the weight ratio outside the range of 0.15 to 0.30. The 20 wt% loading of cobalt catalysts on different spherical silica exhibits nearly similar characteristics. However, the smaller particle of catalyst has a larger surface area and active site, but poor activity. Moreover, the control of the physical and morphology of support has effect on the performance of Co catalysts in CO₂ hydrogenation.

ACKNOWLEDGMENT

The authors acknowledge the Thailand Research Fund (TRF) and the National Research Council of Thailand (NRCT) for financial support of this project.

REFERENCES

- L.M. Yang, Y.J. Wang, Y.W. Sun, G.S. Luo, and Y.Y. Dai: *J. Colloid Interface Sci.*, **299** (2006) 823.
- Y. Yamada, K. Yano: *Micropor. Mesopor. Mater.* **93** (2006) 190.
- Z. Zhang, L. Yang, Y. Wang, G. Luo, and Y. Dai: *Micropor. Mesopor. Mater.* **115** (2006) 447.
- W. Stöber, A. Fink: *J. Colloid Interface Sci.*, **26** (1968) 62.
- Y. Borodko, G.A. Somorjai: *Appl. Cat. A* **186** (1999) 355.
- H. Li, J. Li, H. Ni, and D. Song: *Catalysis letters* **110** (2006) 71



PAPER ACCEPTANCE NOTICE

Dear Bunjerd Jongsomjit,

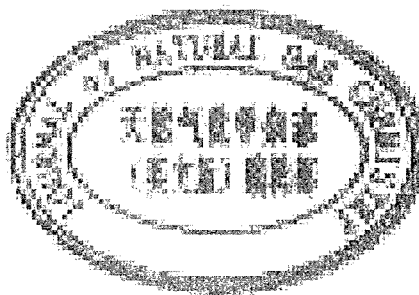
We are honored to notify you that your manuscript entitled "Investigation of Ti-Si composite oxide-supported cobalt catalysts over CO₂ hydrogenation", by "Jakrapan Janlamool, Piyasan Prasertthdam and Bunjerd Jongsomjit", has been accepted for publication in the Journal of Natural Gas Chemistry.

Thank you very much for your support to the journal.

Sincerely yours,

Hong Yang

Hong Yang
Director of Editorial Office
Journal of Natural Gas Chemistry
Dalian Institute of Chemical Physics
Chinese Academy of Sciences
Tel: +86-411-84379237
Fax: +86-411-84379600
jngc@dicp.ac.cn
2011-05-30



Investigation of Ti-Si composite oxide-supported cobalt catalysts over CO₂ hydrogenation

Jakrapan Janlamool, Piyasan Praserttham and Bunjerd Jongsomjit*

Center of Excellence on Catalysis and Catalytic Reaction Engineering,

Department of Chemical Engineering, Faculty of Engineering

Chulalongkorn University, Bangkok 10330, Thailand

*Corresponding author, Tel.: 662-2186869, Fax: 662-2186877

E-mail: bunjerd.j@chula.ac.th

Abstract

In the present work, the different silica-based supported cobalt (Co) catalysts were synthesized and used for CO₂ hydrogenation under methanation. The different supports, such as SSP, MCM41, TiSSP, and TiMCM were used to prepare Co catalysts having 20 wt% of Co loading. The supports and catalysts were characterized by means of N₂ physisorption, XRD, SEM/EDX, XPS, TPR, and CO chemisorption. It was found that after calcination of catalysts, the Ti was present in the anatase form. The introduction of Ti can play important roles on the properties of Co catalysts by; (i) facilitating the reduction of Co oxides species strongly interacted with support, (ii) preventing the formation of silicate compounds, and (iii) inhibiting the RWGS reaction. Based on CO₂ hydrogenation, the CoTiMCM exhibited the highest activity and stability.

Keywords: CO₂ hydrogenation; titania-silica; cobalt catalysts; methanation

1. Introduction

Global warming caused by CO₂ emitted into the atmosphere has become recently a serious problem all over the world. Among the various types of methods for recovering, the chemical fixation of emitted CO₂ is also expected to help the conservation of fossil fuels. Hydrogenation of CO₂ to methane is important in the purification of ammonia feedstocks, methanation of coal-derived gases and the production of process heat from reclaimable waste streams containing carbon dioxide [1]. Development of catalysts for CO and CO₂ hydrogenation is the key technology of gas to liquid (GTL) process. The catalytic hydrogenation of carbon monoxide and carbon dioxide produces a large variety of products ranging from methane and methanol to higher molecular weight alkanes, alkenes and alcohols [2-5]. The methanation of CO₂ is reported to proceed with a lower activated energy than the methanation of CO [6]. The lower exothermicity of the overall reaction of CO₂ as compared to CO makes temperature control in a catalytic reactor easier as shown in equation (1) and (2) [7].



Transition metal oxides are generally regarded as good hydrogenation catalysts. Furthermore, Weatherbee and Bartholomew [8] studied the specific activity of various Group VIII metals catalysts supported on SiO₂ on the methanation of CO₂ at 177-377°C and 140-1030 kPa and found that the activity decreased in the order of Co > Ru > Ni > Fe. The Co and Ni-based catalysts were preferred because they required considerably milder operating pressures (about 1 atm) than the high pressure reactor for the Fe catalyst [9]. Supported cobalt catalysts were the preferred catalysts for CO₂ hydrogenation because of lower cost compared to Ru [10]. Moreover, the catalytic activity of metal towards carbon deposition was found to decrease in order Ni > Co > Fe [11,12]. The previous research revealed that supports, such as

Al_2O_3 , SiO_2 , ZrO_2 , TiO_2 and CeO_2 can efficiently affect activity and selectivity of cobalt catalysts for CO and CO_2 hydrogenation [13-16]. Recently, the Ti-Si composite represents a novel class of materials that was attractively used as catalysts and supports for a wide variety catalytic reaction. It was reported that the photocatalytic activity of Ti-Si is 3-fold higher than the corresponding TiO_2 [17–19]. Furthermore, heterogeneous catalysts such as SiO_2 -supported TiO_2 and Ti-Si composite are known to be effective for selective oxidation reaction [20]. The Ti-Si composite supports exhibit the novel properties that are not finding in single oxide supports. In addition, mesoporous SiO_2 , such as MCM41 and hexagonal mesoporous silica (HMS), exhibits sufficiently high surface area, thermal stability, excellent mechanical strength and uniform pore sizes [21]. The Ti-Si composite is generally synthesized by flame hydrolysis [22], impregnation [23], coprecipitation [24] and sol-gel [25] methods by adding titanium precursor into silica framework. The titanium distribution in the Ti-Si composite depends on the method of preparation [26]. The sol-gel hydrolysis is most widely used because of capability in controlling the textural and surface properties of the mixed oxides [21].

The present research focuses on application of the Ti-Si composite used as support for cobalt catalysts. First, the mesoporous silicas, such as spherical silica particle (SSP) and MCM41 were prepared. Then, titanium isopropoxide was introduced into the silica framework by hydrolysis to obtain the Ti-Si composite. The cobalt catalysts were prepared by direct impregnation of cobalt precursor onto different supports. The characteristics and catalytic behaviors via CO_2 hydrogenation were investigated and further discussed in more detail.

2. Experimental

2.1 Materials

Chemicals as follows were used; titanium isopropoxide [97% TiPOT (Aldrich)], tetraethyl orthosilicate [98% TEOS (Aldrich)], ammonia [30% (Panreac)], ethanol [99.99% (J.T. Baker)], cetyltrimethylammonium bromide [CTAB (Aldrich)], isopropanol (QReC), cobalt (II) nitrate hexahydrate [98% $\text{Co}(\text{NO}_3)_2 \cdot 6\text{H}_2\text{O}$ (Aldrich)].

2.2 Support and cobalt catalyst preparation

The mesoporous silica supports were synthesized by the sol-gel method. The composition of the synthesis gel was as follows; molar ratio: 1 TEOS : 0.3 $\text{C}_{16}\text{TMABr}$: 11NH_3 : x ethanol : 144 H_2O . Molar ratio of ethanol addition was varied at 0 for MCM41 and at 58 for SSP [27]. The mixture was further stirred for 2 h at room temperature. The white precipitate was then collected by filtration and washed with deionized water. The dried sample was calcined at 550°C for 6 h with a heating rate of 10°C/min in air.

The desired amount of titanium isopropoxide (ca. 25 wt% of Ti) was dissolved in isopropanol (1:3 w/w). The SSP or MCM41 was then added into the solution mixture and stirred for 1 h. Hydrolysis was performed by addition of ammonia (H_2O : TiPOT at 4:1). The sol was further stirred for 20 h at room temperature. Then, the sample was dried at 110°C for 24 h. Finally, the samples were calcined at 850°C for 2 h in a muffle furnace.

The cobalt catalysts having 20 wt% of Co were prepared by the incipient wetness impregnation using aqueous solution of cobalt (II) nitrate hexahydrate [$\text{Co}(\text{NO}_3)_2 \cdot 6\text{H}_2\text{O}$]. The catalysts were dried at 110°C for 12 h, and then calcined in air at 500°C for 4 h.

Nomenclature of sample is given as follows; SSP and MCM refer to spherical silica and MCM-41, respectively. Furthermore, TiSSP and TiMCM refer to titania-spherical silica

composite and titania-MCM-41 composite, respectively. For catalysts samples, CoX refers to cobalt catalyst supported on the X support as mentioned above.

2.3 Catalyst characterization

The various supports and cobalt catalysts were characterized by several techniques as follows;

N₂ physisorption: N₂ physisorption (N₂ adsorption at -196 °C in a Micromeritics ASPS 2020) was performed to determine surface areas of the various supports and cobalt catalysts.

X-ray diffraction (XRD): XRD was used to determine the phase composition of the different supports and catalysts using SIEMENS D 5000 X-ray diffractometer with CuK α radiation with Ni filter in the 2 θ range of 20-80 degrees with resolution of 0.04°.

Temperature programmed reduction (TPR): TPR was used to determine the reducibility and reduction temperature of the cobalt catalysts. Approximately, 0.05 g of catalyst sample was used in the operation and temperature ramping from 35°C to 800°C at 10 °C/min. The carrier gas was 10 % H₂ in Ar. A thermal conductivity detector (TCD) was used to measure the amount of hydrogen consumption. The calibration of hydrogen consumption was performed with bulk cobalt oxide (Co₃O₄) at the same condition.

CO chemisorption: The static CO chemisorption at room temperature on the reduced catalysts was used to determine the number of reduced surface cobalt metal atoms. CO chemisorption was carried out following the procedure using a Micromeritics Pulse Chemisorb 2750 instrument. Prior to chemisorption, the catalysts were reduced at 350°C for 3 h after ramping up at a rate of 10°C/min. After that, 30 μ l of carbon monoxide was injected into catalyst and repeated until the desorption peaks were constant at room temperature. Amounts of carbon monoxide adsorption on catalyst are proportional to the number of active sites.

Scanning electron microscopy (SEM) and dispersive X-ray spectroscopy (EDX): SEM (JEOL mode JSM-5800LV) and EDX (Link Isis Series 300) were used to determine the morphology and elemental distribution of the catalyst particles. The particle size and cobalt distribution of catalyst samples was observed using JEOL-JEM 200CX transmission electron microscope operated at 100 kV.

X-ray photoelectron spectroscopy (XPS): The XPS analysis was performed originally using an AMICUS spectrometer equipped with a Mg K $_{\alpha}$ X-ray radiation. For a typical analysis, the source was operated at voltage of 15 kV and current of 12 mA. The pressure in the analysis chamber was less than 10⁻⁵ Pa.

2.4 Reaction test

CO₂ hydrogenation was performed to determine the overall activity and selectivity of the catalysts. Typically, 0.1 g of catalyst was packed in a fixed-bed microreactor. The catalyst sample was reduced *in situ* in flowing H₂ (50ml/min) at 350°C for 3 h. After reduction, a flow rate of Ar = 8 ml/min, 8.8% CO₂ in H₂ = 22 ml/min was fed into the reactor. The CO₂ hydrogenation was carried out at 220°C at 1 atm. The product gas samples were taken in 1 h interval and analyzed by gas chromatography. The steady state was reached within 6 h.

3. Results and Discussion

3.1 Characteristics

The surface areas of the different supports and catalysts are shown in **Table 1**. The surface areas the mesoporous silicas (SSP and MCM41) are remarkably high as expected. However, with the addition of Ti into the silica framework, it was found that of Ti-Si composites (TiSSP and TiMCM) were much lower than the corresponding mesoporous silica.

As seen, the surface areas of TiSSP and TiMCM calcined at 850°C were dramatically low ca. 385 and 137 m²/g, respectively. This was due to the distribution of Ti in the silica framework. The surface areas of cobalt catalysts deposited on SSP and MCM41 were much less than their supports, whereas the CoTiSSP and CoTiMCM had only slight effect. This can be attributed to the larger pore sizes of CoSSP and CoMCM. The phase identification was carried out on the basis of data obtained from XRD. The XRD patterns for all support samples are shown in **Figure 1**. As seen, the SSP and MCM41 exhibited the broad peak at 20-30° indicating amorphous silica. The Ti-Si composites for both TiSSP and TiMCM showed the XRD patterns for titania being present in the anatase form (2θ of 25.3, 37.8, 48, 54, 55 and 75°). The XRD patterns of the calcined Co catalysts are shown in **Figure 2**. All catalyst samples exhibited almost identical XRD patterns of Co₃O₄ at 31°, 37°, 45°, 59°, and 65° [28]. It can be observed that the XRD peaks of anatase TiO₂ at 2θ of 25.3° was less apparent due to XRD peaks of Co₃O₄ displayed the strong intensity resulting in hindrance the observation of anatase peaks.

TPR was performed in order to determine the reduction behaviors. The TPR profiles of all catalysts are shown in **Figure 3**. The reduction temperatures for all calcined catalysts were located between ca. 200 to 600 °C. The one broad reduction peak with shoulder was observed for all catalysts. This can be generally assigned to the overlap of two step reduction of Co₃O₄ to CoO and then to Co⁰. The two reaction steps [equation (3) and (4)] may not be observed depending upon the TPR conditions, such as ramping rate of temperature, feed gas flow rate, and amount of samples.



The reduction temperature and reducibility results are summarized in **Table 2**. The reduction temperatures of CoSSP and CoMCM were located at ca. (210-330°C) and (210-360°C), respectively. For the CoTiSSP and CoTiMCM, the reduction temperatures were shifted over the broad range (220-610°C for CoTiSSP and 220-600°C for CoTiMCM) indicating larger number of reduced cobalt atoms. The higher reduction temperature represented the cobalt oxide species strongly interacted with the support, which are reducible. Therefore, the presence of Ti into the silica frame work apparently facilitated the reduction of strongly interacted cobalt with the support. Without introduction of Ti, the higher reduction peak was absent as seen for CoSSP and CoMCM samples. The strong interaction between cobalt and supports was reported within the order of $\text{Al}_2\text{O}_3 > \text{TiO}_2 > \text{SiO}_2$ [29]. In addition, the reducibilities of CoTiSSP and CoTiMCM catalysts were higher than those of CoSSP and CoMCM catalysts due to the reduction of strongly interacted cobalt oxide species as mentioned earlier. It was also reported that the use of TiPOT for the preparation of Ti-Si composite also resulted in increased reducibility of nickel catalysts [26].

The CO chemisorption was conducted on samples reduced in hydrogen flow at 350°C for 3 h. The amounts of carbon monoxide adsorbed on the catalysts were determined in order to obtain the number of reduced cobalt metal atoms. The adsorbed amounts of CO were directly proportional to the active site. The amounts of CO adsorbed on the catalytic phase were ranged between 19 to 37 $\mu\text{mol CO/g}$ of catalysts as also shown in **Table 2**. It can be observed that in this case, the TPR and CO chemisorption results did not relate due to different conditions applied. The CO chemisorption results showed that the number of reduced cobalt metal atoms slightly decreased with the presence of titania in the support. This was in accordance with the decreased number of cobalt atoms with increasing the amounts of titania in the mixed oxide supports [30]. Furthermore, the acidic properties of titania-silica were quite different from that of either pure titania or pure silica, since pure titania only

possesses Lewis acidity while silica has neither Bronsted nor Lewis acidity. However, new Bronsted acid sites are created when titania and silica form Ti-O-Si chemical bonds [31-33]. One possible reason for the lower CO chemisorption of CoTiSSP and CoTiMCM can be explained based on the electron donor additives like alkali metals enhance chemisorption, while electron acceptors inhibit chemisorption [34-36]. It should be noted that the results from CO chemisorption are different from those with TPR due to differences in measurement conditions for both techniques.

SEM and EDX were also conducted in order to study the morphologies and elemental distribution of the catalysts, respectively. The typical external surface granule and EDX mapping of the calcined cobalt catalysts are shown in **Figure 4a-4d**. It can be observed that the cobalt oxide species exhibited good distribution. The white spots on the external surfaces represent high concentrations of Co. The EDX analysis is not a bulk technique, but rather a surface analytical tool based on the fact that it gives information down to a depth of approximately 1 μm from the surface that makes the type of information obtained with EDX comparable to atomic absorption [37]. **Table 3** summarizes the element quantities of cobalt catalysts based on EDX and XPS analysis. It should be mentioned that EDX only measures the concentrations in a layer less than 1 μm from the surface. The EDX results revealed that the Ti loading was at 17.4 and 23.1 wt% for CoTiSSP and CoTiMCM, respectively. In addition, the Co loading for all catalysts were ranged between 22 and 30 wt%. The element composition of surface and subsurface layers (depth of XPS analysis is about ten angstrom) indicated that the amounts of Ti were at 43 and 31 wt% for CoTiSSP and CoTiMCM, respectively. The amounts of Ti from XPS analysis were higher than those obtained from EDX analysis. This was due to the titania accumulated on the external surface of silica supports. Moreover, the amounts of Co for CoMCM, CoTiSSP and CoTiMCM from XPS analysis were distinctly higher than EDX analysis indicating that the cobalt oxides distributed

mostly on the external surface. In contrast, the amounts of Co for CoSSP from XPS measurement were remarkably less than that obtained from the EDX analysis. This was confirmed the cobalt oxides dispersed mostly in the bulk of silica particles.

Besides the determination of surface concentration, XPS is one of the most powerful techniques used to identify the binding energy (BE) for elements. Considering the resulting BE obtained from XPS as also shown in **Table 3**, it can be observed that the Co 2p core level spectra of Co₃O₄ were present at the BE of 780-782 eV and 795-796 eV for 2p_{3/2} and 2p_{1/2}, respectively in all catalyst samples. These values were in agreement with the other work [38]. On the other hand, no change in BE for Co 2p core level with the present of Ti. However, the CoSSP and CoMCM exhibited the BE at 95.1 and 94.6 eV and 104.2 and 103.5 eV, respectively. In fact, the BE at 95.1 and 94.6 eV were assigned to the formation of silicate compounds as also reported by Wagner et al.[39] and Arnby et al.[40]. Previous reports suggested that the formation of surface cobalt silicates during preliminary steps of catalyst preparation, or even during reduction, was considered as a reason for partial reduction of the total cobalt present at the temperatures normally used up to 500°C [41]. However, the presence of Ti in CoTiSSP and CoTiMCM apparently resulted in the absence of the BE for silicate compound. These results are in accordance with those obtained from TPR.

The TEM micrographs for all catalysts are shown in **Figure 5 (a-d)**. The dark spots represented cobalt oxide patches dispersing on the supports after calcination of catalysts. **Figure 5 (a, b)** shows that the cobalt oxide species exhibited good distribution in the CoSSP and CoTiSSP catalysts, respectively. **Figure 5 (c)** reveals that cobalt oxide species are agglomerated in CoMCM catalyst. In contrast, **Figure 5 (d)** displays the cobalt oxide species having good distribution in the CoTiMCM catalyst. The TEM micrographs demonstrated that the titania particle on the MCM41 can improve the dispersion of cobalt oxide. This phenomenon was also observed with the presence of Ti in Ni catalyst [26].

3.2 Reaction study

The CO₂ hydrogenation over different cobalt catalysts at 220°C under methanation condition was investigated. The reaction results are summarized in **Table 4**. Methane is a major product for all catalyst samples. It was found that the CoTiMCM sample exhibited the highest activity among other samples. The CO selectivity also decreased with the presence of Ti in MCM41 due to increased acidity with increasing the amount of Ti in the supports [26]. This is in agreement with the increased amount of absorbed CO₂ with increasing basicity of the alkali metal oxides, which might be related to the influence on the local electron density of neighboring metal species [7]. In addition, the stability of catalyst was found to increase with the presence of Ti when compared the conversion of initial and steady-state. The obtained products for methane and CO indicate that CO₂ hydrogenation on these catalysts occurred via a consecutive mechanism as shown in equation (5) and (6). CO₂ is first converted to CO by the reverse water gas-shift (RWGS) reaction, and then CO was hydrogenated to methane.



For CO₂ hydrogenation, the operating temperature must be rather high because of the equilibrium constraints for the reverse CO shift reaction. This limits the application of temperature in the lower range for Fischer-Tropsch conversion [7]. In this study, the activities for cobalt catalysts were not related to the cobalt dispersion obtained from CO chemisorption. This was in accordance with the methanation turnover rates in Fischer-Tropsch synthesis that

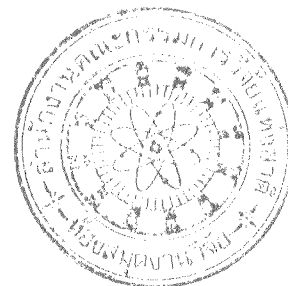
were also independent of cobalt dispersion on supported catalysts and surface orientation on Co single crystals [42].

4. Conclusion

In summary, the addition of Ti on SSP and MCM41 can alter the characteristics and catalytic properties of CoTiSSP and CoTiMCM catalysts. It was found that the presence of Ti can facilitate the reduction of cobalt oxide species strongly interacted with the support resulting in the observation of high temperature reduction peak. Based on XPS analysis, it was observed that the silicate formation was disappeared with the presence of Ti. It is worth noting that the CoTiMCM catalyst exhibited the highest activity for CO₂ hydrogenation due to increased reducibility. The addition of Ti also inhibited the RWGS leading to decreased CO selectivity.

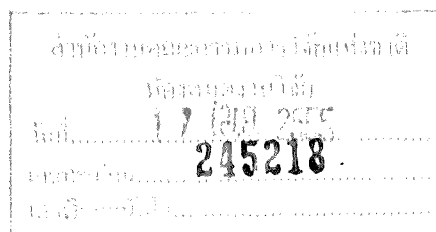
Acknowledgement

The authors thank the Thailand Research Fund (TRF) and Office of the Higher Education Commission (CHE), the National Research Council of Thailand (NRCT), and NRU-CU (AM1088A) for the financial support of this project.



References

- [1] Weatherbee GD, Bartholomew CH. *J Catal* 1982, **77**: 460
- [2] Somorjai GA. *Introduction to Surface Chemistry and Catalysis*, New York: Wiley. 1994
- [3] Dry ME. *Appl Catal A-Gen*, 1996, **138**: 319
- [4] Adesina AA. *Appl Catal A-Gen*, 1996, **138**: 345
- [5] Iglesia E. *Appl Catal A-Gen*, 1997, **161**: 59-78
- [6] Peebles DE, Goodman DW, White JM. *J Phys Chem*, 1983, **87**: 4378
- [7] Riedel R, Michael C, Hans S, Georg S, Sang SN, Ki WJ, Myoung JC, Gurram K, Kyu WL. *Appl Catal A-Gen*, 1999, **186**: 201
- [8] Weatherbee G.D. and Bartholomew C.H., *J Catal*, 1984, **87** : 352
- [9] Anderson RB, *The Fischer-Tropsch Synthesis*, New York: Academic Press, 1984
- [10] Jongsomjit B, Panpranot J, Goodwin JG, *J Catal*, 2001, **204** : 98–109
- [11] Khavrus VA, Lemesh NV, Gordeichuk SV, Tripolskii AI, Ivashchenko TS, Strizhak PE, *Theor Exp Chem*, 2006, **42** : 234–239
- [12] Khavrus VO, Lemesh NV, Gordijchuk SV, Tripolsky AI, Ivashchenko TS, Biliy MM, Strizhak PE, *React Kinet Catal Lett*, 2008, **93** : 295–303
- [13] Ruiz AG, Ramos IR. *React Kinet Catal Le*, 1985, **23**: 93
- [14] Suo Z, Kou Y, Niu J, Zhang W, Wang H. *Appl Catal A-Gen*, 1997, **148**: 301
- [15] Storsaeter S, Totdal B, Walmsley JC, Tanem BS, Holmen A. *J Catal*, 2005, **236**: 139
- [16] Zhao Z, Yung MM, Ozkan US. *Catal Commun*, 2008, **9**: 1465
- [17] Anderson C, Bard AJ. *J Phys Chems*, 1995, **99**: 9882
- [18] Ruetten SA, Thomas JK, *Photoch Photobiol Sci*, 2003, **2**: 1018
- [19] Chun H, Yizhong W, Hongxiao T. *Appl Catal B- Environ*, 2001, **30**: 277
- [20] Liu Z, Crumbaugh GM, Davis RJ. *J Catal*, 1996, **159**: 83
- [21] Gao X, Wachs IE. *Catal Today*, 1999, **51**: 233



- [22] Schultz PC, *J Am Ceram Soc*, 1976, **59**: 214
- [23] Yoshida S, Takenaka S, Tanaka T, Hirano H, Hayashi H, Eleventh International Congress on Catalysis, *Stud Sur Sci Catal*, 1996, **101**: 871
- [24] Itoh M, Hattori H, Tanabe K. *J Catal*, 1974, **35**: 225.
- [25] Ohno T, Tagawa S, Itoh H, Suzuki H, Matsuda T. *Mater Chem Phys*, 2009, **113**: 119
- [26] Grzechowiak JR, Szyszka I, Masalska A. *Catal Today*, 2008, **137**: 433
- [27] Liu S, Collart O, Cool P, VanDerVoort P, Vansant EF, Minhua J, Lebedev OI, VanTendeloo G. *Phys Chem B*, 2003, **107**: 10405.
- [28] Rojanapipatkul S, Jongsomjit B, *Catal Commun*, 2008, **10**: 232
- [29] Jacobs G, Das TK, Zhang Y, Li J, Racoillet G, Davis BH, *Appl Catal A-Gen*, 2002, **233**: 263
- [30] Jongsomjit B, Wongsalee T, Praserttham P. *J. of Mater Chem Phys*, 2006, **97**: 343
- [31] Liu ZF, Tabora J, Davis RJ, *J Catal*, 1994, **149**:117
- [32] Molnar A, Bartok M, Schneider M, Baiker A, *Catal Lett*, 1997, **43**: 123
- [33] Doolin PK, Alerasool S, Zalewski DJ, Hoffman JF, *Catal Lett*, 1994, **25**: 209
- [34] Rhodin TN, Brucker CF, *Solid State Commun*. 1977, **23**: 275
- [35] Queau R, Labroue D, Poilblanc R, *J Catal*, 1981, **69**: 249
- [36] Benziger J, Madix RJ, *Surf Sci*, 1980, **94**: 119
- [37] Duran JDG, Guindo MC, Delgado AV, Caballero FG. *J Colloid Interface Sci*, 1997, **193**: 223
- [38] Morales F, De Groot FMF, Gijzeman OLJ, Mens A, Stephan O, Weckhuysen BM, *J Catal*, 2005, **230**: 301
- [39] Wagner CD, Naumkin AV, Vass AK, Allison JW, Powell CJ, Rumble JR. NIST X-ray Photoelectron Spectroscopy Database, Version 3.4, 2004.

- [40] Arnby K, Rahmani M, Sanati M, Cruise N, Carlsson AA, Skoglundh M. *Appl Catal B-Environ*, 2004, **54**: 1
- [41] Van SE, Sewell GS, Makhothe RA, Micklethwaite C, Manstein H, De Lange H, O'Connor CT, *J Catal*, 1996, **162**: 220
- [42] Johnson BG, Bartholomew CH, Goodman DW. *J Catal*, 1991, **128**: 231

Table 1 BET surface area, pore volume and pore diameter of supports and cobalt catalysts.

Samples	A _{BET} (m ² /g)	V _p (cm ³ /g)	D _{BJH} (nm)
SSP	927	0.8135	2.04
MCM	1187	1.0287	2.13
TiSSP	385	0.1587	3.23
TiMCM	137	0.1371	4.57
CoSSP	637	0.4898	2.26
CoMCM	583	0.2134	2.58
CoTiSSP	380	0.2117	2.82
CoTiMCM	126	0.1004	4.24

Table 2 Maximum temperatures, reducibility from TPR profiles and Co dispersion of cobalt catalysts.

Catalysts	Reduction Temperature (°C)	Reducibility ^a (%)	Total CO chemisorption μmol CO/g.cat	% dispersion of cobalt ^b
CoSSP	210-330	30.3	28	0.84
CoMCM	210-360	21.2	37	1.10
CoTiSSP	220-610	45.4	21	0.61
CoTiMCM	220-600	45.5	19	0.56

^a Determined by TPR analysis^b Determined by CO chemisorption

Table 3 XPS data and EDX analysis of cobalt catalysts.

Catalysts	BE for	BE for	BE for	Amount of element			Amount of element		
	Si	Ti	Co	at surface(%mass) ^a			at bulk (%mass) ^b		
	2p(eV)	2p(eV)	2p(eV)	Si	Ti	Co	Si	Ti	Co
CoSSP	95.10		781.00	90.66	-	9.34	75.51	-	24.29
	104.20	-	795.80						
CoMCM	94.60		780.20	59.79	-	40.22	69.65	-	30.35
	103.50	-	795.30						
CoTiSSP	103.70	460.05	781.00	19.80	42.55	37.64	60.49	17.41	22.10
		465.65	796.60						
CoTiMCM	103.40	459.65	780.40	34.02	30.63	35.35	46.11	23.08	30.81
		465.55	795.40						

^a Determined by XPS analysis^b Determined by EDX analysis

Table 4 Activity and product selectivity of cobalt catalysts.

Reaction temperature (°C)	Catalysts	Conversion ^a		Rate ^c (x10 ² g CH ₂ /g cat.h)	Product selectivity ^c (%)	
		Initial ^b	Steady state ^c		CH ₄	CO
220	CoSSP	38	27	16.5	89.5	10.5
	CoMCM	35	28	18.1	91.4	8.6
	CoTiSSP	17	16	10.0	92.1	7.9
	CoTiMCM	35	34	22.3	94.9	5.1

^a CO₂ hydrogenation was carried out at 1 atm, and H₂/CO₂/Ar = 20/2/8, F/W= 18 L/g cat.h.

^b After 5 min of reaction.

^c After 6 h of reaction.

List of Figure

Figure 1 XRD patterns of different supports

Figure 2 XRD patterns of different cobalt catalysts

Figure 3 TPR profiles of different cobalt catalysts

Figure 4 SEM micrographs and EDX mapping of cobalt catalysts (a) CoSSP, (b) CoMCM, (c) CoTiSSP, (d) CoTiMCM.

Figure 5 TEM micrographs of cobalt catalysts (a) CoSSP, (b) CoMCM, (c) CoTiSSP, (d) CoTiMCM.

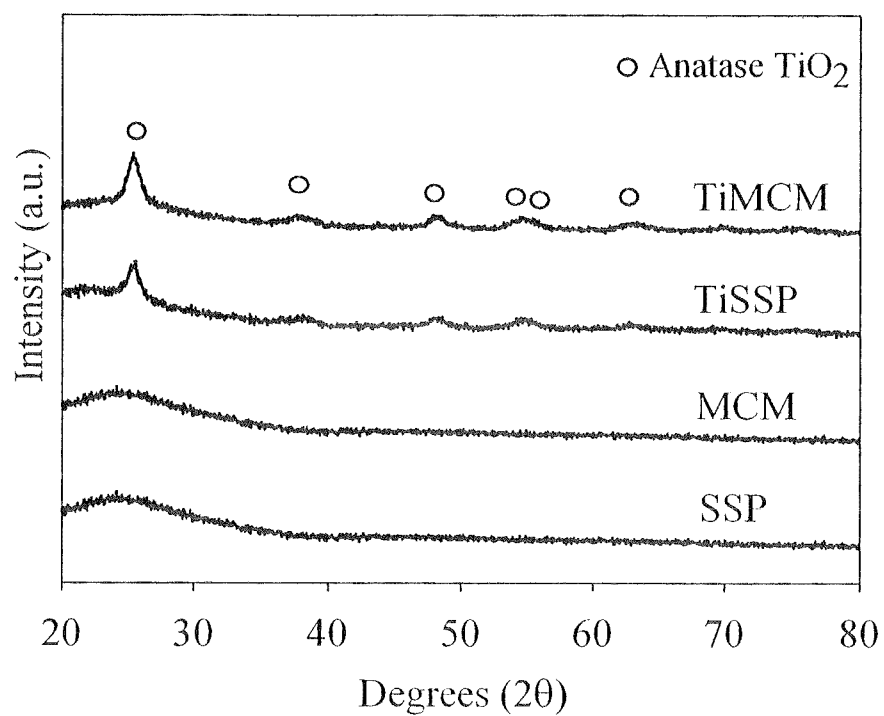


FIGURE 1

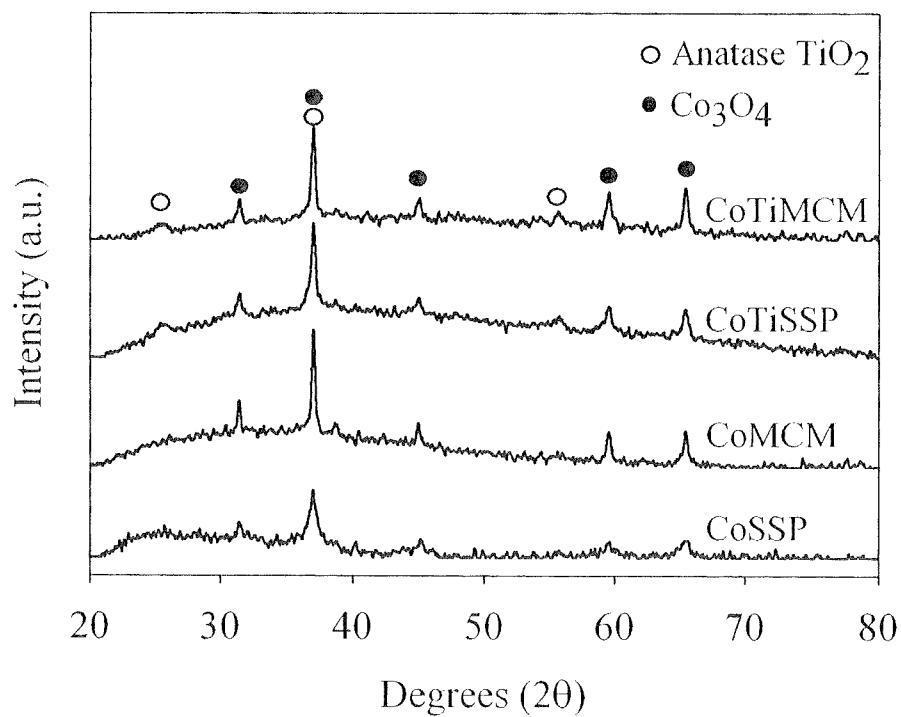


FIGURE 2

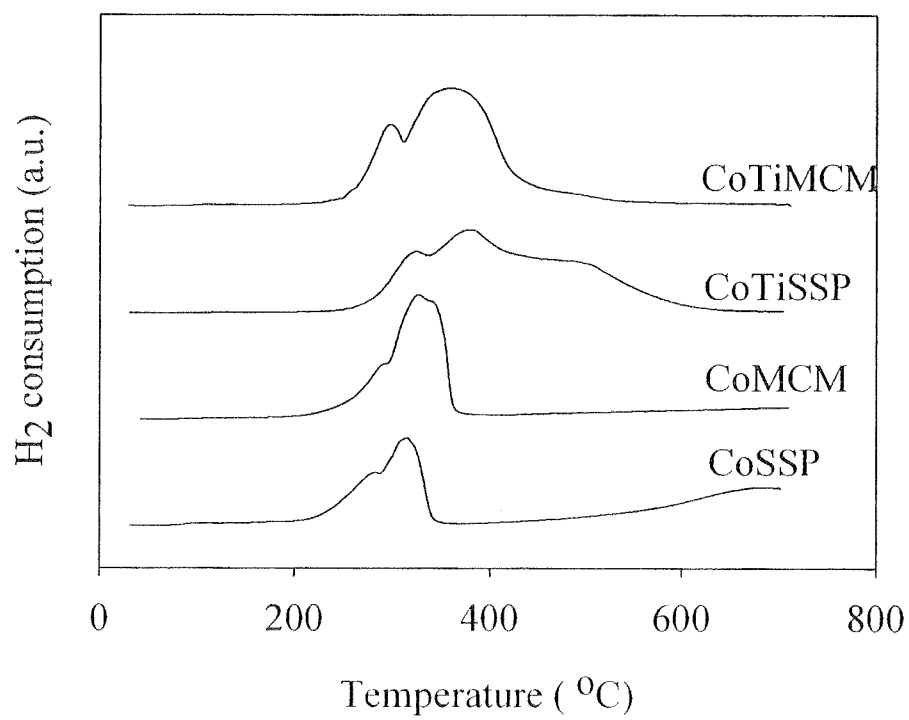


FIGURE 3

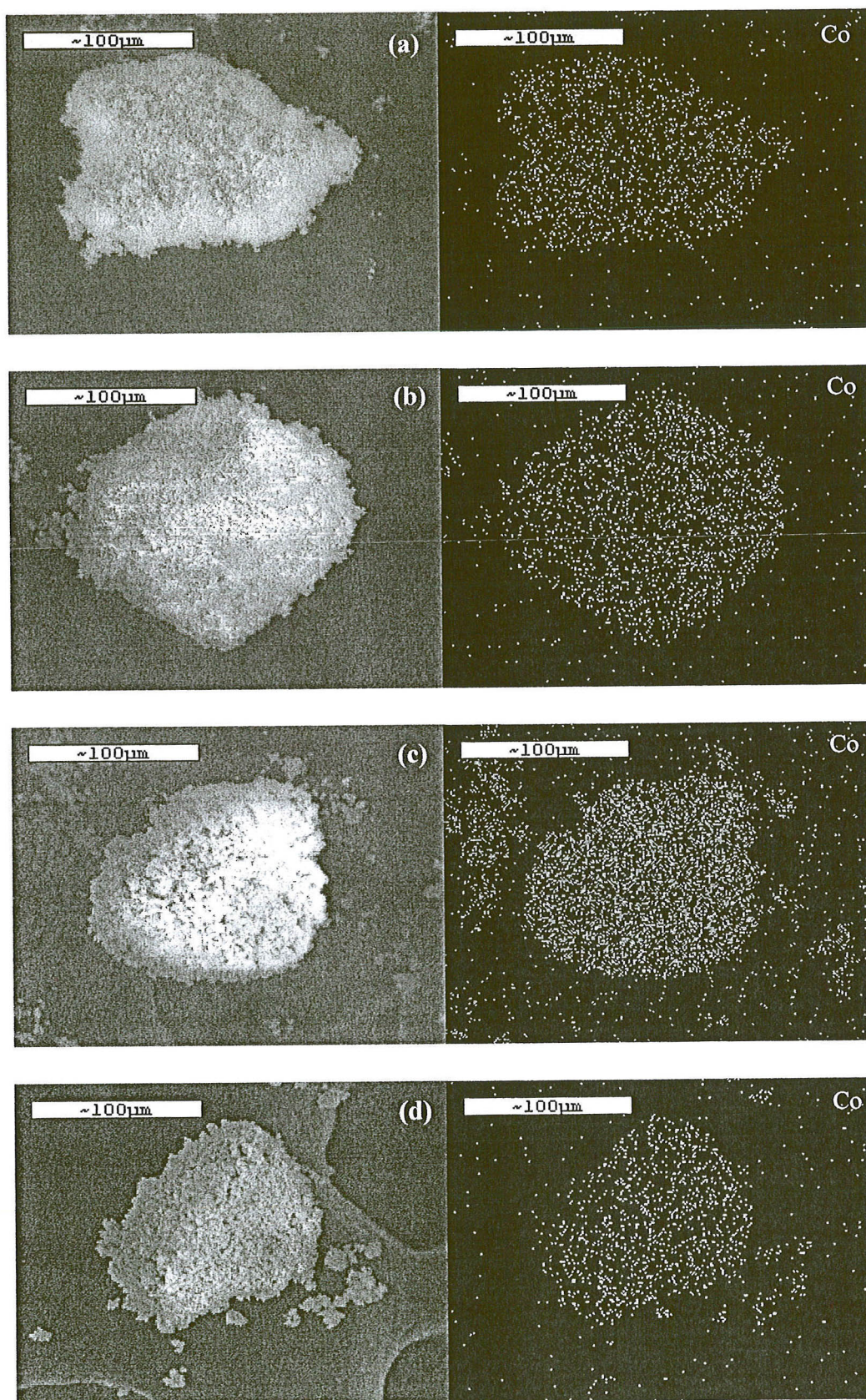


FIGURE 4

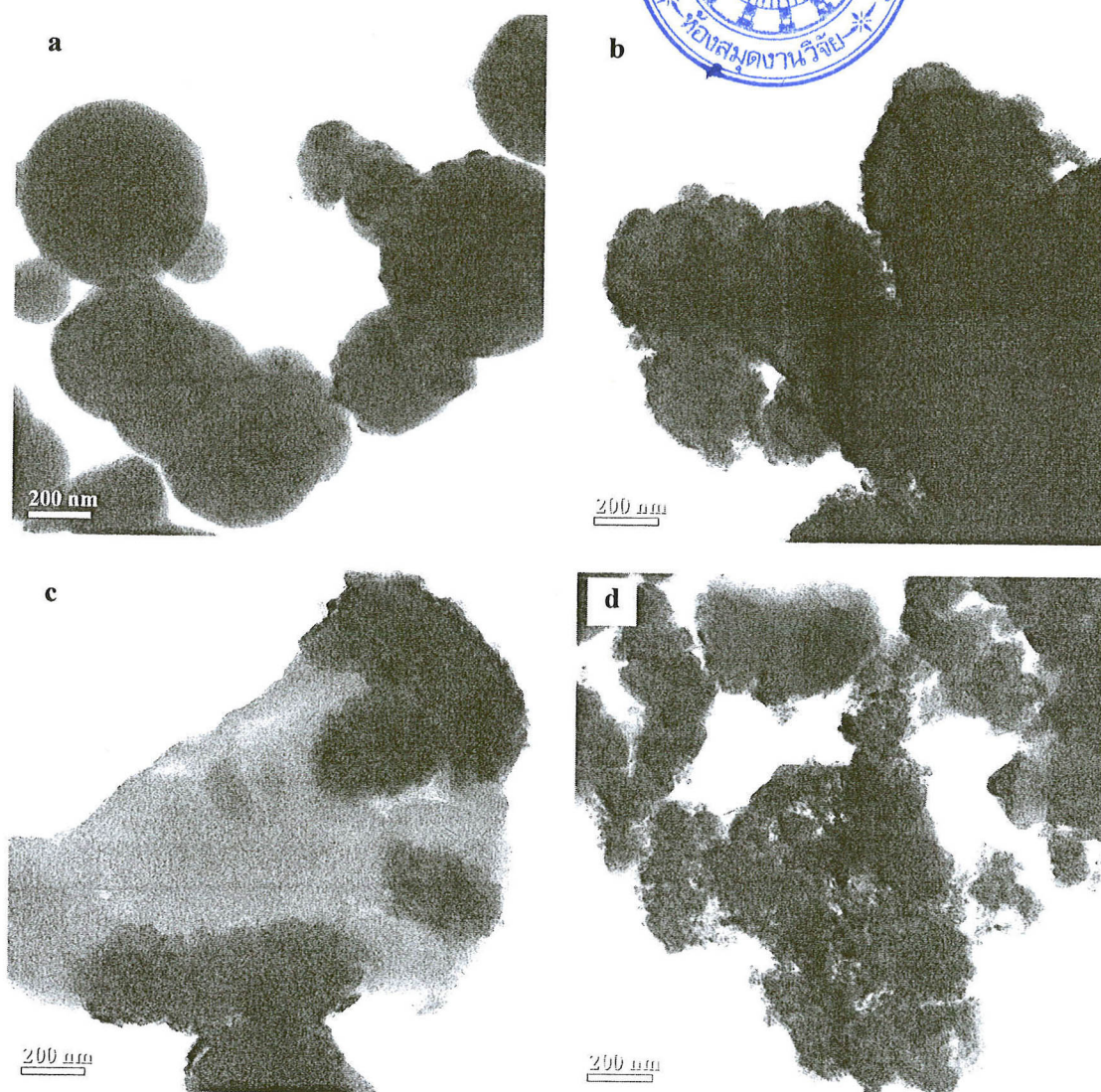


FIGURE 5